JVSTA Journal of Vacuum Science & Technology A

Aluminum-doped zinc oxide formed by atomic layer deposition for use as anodes in organic light emitting diodes

Su Cheol Gong, Yong-June Choi, Hyuncheol Kim, Chang-Sun Park, Hyung-Ho Park, Ji Geun Jang, Ho Jung Chang, and Geun Young Yeom

Citation: Journal of Vacuum Science & Technology A **31**, 01A101 (2013); doi: 10.1116/1.4738749
View online: http://dx.doi.org/10.1116/1.4738749
View Table of Contents: http://scitation.aip.org/content/avs/journal/jvsta/31/1?ver=pdfcov
Published by the AVS: Science & Technology of Materials, Interfaces, and Processing

Aluminum-doped zinc oxide formed by atomic layer deposition for use as anodes in organic light emitting diodes

Su Cheol Gong, Yong-June Choi, Hyuncheol Kim, Chang-Sun Park, and Hyung-Ho Park[a)]
Department of Materials Science and Engineering, Yonsei University, Seoul 120-749, South Korea

Ji Geun Jang and Ho Jung Chang
Department of Electronics Engineering, Dankook University, Cheonan-si, Chungcheongnam-do 330-714, South Korea

Geun Young Yeom
Department of Materials Science and Engineering, Sungkyunkwan University, Suwon, Kyunggi-do 440-746, South Korea

(Received 26 April 2012; accepted 9 July 2012; published 26 July 2012)

Aluminum-doped zinc oxide films produced by atomic layer deposition were investigated for use as anodes in organic light emitting diode (OLED) devices. Al-doped ZnO (AZO) films (~200 nm thick) were deposited at temperatures of 200, 230, and 260 °C and the AZO film deposited at 260 °C demonstrated carrier mobility, carrier concentration, resistivity, and transmittance values of 16.2 $cm^2\,V^{-1}\,s^{-1}$, $5.18\times10^{20}\,cm^{-3}$, $7.34\times10^{-4}\ \Omega\,cm$, and 90%, respectively. OLED devices with a DNTPD/TAPC/$Bebq_2$:10% doped RP-411/Bphen/LiF/Al structure on a glass substrate fabricated using an AZO anode formed at 260 °C showed turn-on voltage, maximum luminance, and current efficiency values of 5.3 V, 16680 cd/m^2, and 4.8 cd/A, respectively. © *2013 American Vacuum Society*. [http://dx.doi.org/10.1116/1.4738749]

I. INTRODUCTION

Currently, indium tin oxide (ITO) is the most widely used transparent conducting oxide (TCO) as an electrode material for optoelectronic devices because of its excellent features, low electrical resistivity ($\sim2\times10^{-4}\ \Omega\,cm$), high transparency (~90%) due to its wide optical bandgap (3.7 eV), and high work function (4.8 eV). However, ITO has many drawbacks, including its chemical instability, potential harm to humans, and high cost due to the relative scarcity of indium.[1,2] Therefore, in recent years new TCOs have been investigated as electrodes for optoelectronic devices in order to replace ITO, which is considered to be one of the key challenges to improve the optoelectronic performance. In particular, among the alternative TCO materials, zinc oxide (ZnO), which is typically an *n*-type semiconductor, is regarded as a good representative material and has excellent features, including high chemical stability, low material cost, high conductivity, and high optical transmittance.[3,4] Moreover, the conductivity and optical transmittance of ZnO can be controlled by impurity doping with an electron donor from various III metal groups such as gallium,[3] indium,[4] and aluminum.[5–19] Of these, Al-doped zinc oxide (AZO) films are considered to be a suitable TCO electrode material for optoelectronic devices.

AZO films can be fabricated using a variety of methods, including pulsed laser deposition (PLD),[5–7] sputtering,[8,9] and sol-gel[10,11] methods. In particular, AZO films deposited by PLD and sputtering methods have demonstrated a low resistivity of under $2.0\times10^{-4}\ \Omega\,cm$ and a high transmittance of over 85% with a wide optical energy bandgap compared to pure ZnO films.[6–8] The possibility of TCO electrodes has been successfully demonstrated in optoelectronic device applications such as organic light emitting diodes (OLEDs),[1,4,9] solar cells,[17] and thin film transistors (TFTs).[10] Recently, a novel deposition technique for AZO films was developed using atomic layer deposition (ALD),[12–19] which is a cost efficient, low temperature deposition process. In addition, the electrical and optical properties of thin films deposited via ALD can be modified easily and exactly by controlling the deposition to under several angstroms per cycle.[20] Consequently, AZO TCOs deposited by the ALD method have been researched for use in optoelectronic devices such as organic solar cells,[17] OLEDs,[18] and TFTs.[19] However, there is still a need for a comparative work with the AZO films deposited by sputtering and PLD methods.

In this work, therefore, we studied AZO films formed by ALD for application in OLED devices in order to ascertain their performance as a TCO anode. The AZO films were deposited on glass substrates at various deposition temperatures ranging from 200 to 260 °C and the variations of the electrical conductivity and optical transmittance as a function of the deposition temperature were analyzed. The prepared AZO films were also tested as a TCO anode in OLED devices. Finally, their luminance and current efficiency characteristics were investigated.

II. EXPERIMENT

The deposition of AZO films was carried out using a flow-type ALD reactor (Lucida D100, NCD). To investigate the effect of the deposition temperature, AZO films were deposited on high optical Corning 1737 glass substrates (>90% transmittance) with dimensions of 2.5 cm × 2.5 cm under different deposition temperatures ranging from 200 to 260 °C under a base pressure of 50 mTorr. AZO films composed of ZnO and AlO_x were formed using a "super cycle"

[a)]Electronic mail: hhpark@yonsei.ac.kr

process of 39 total super cycles where each super cycle was composed of 29 ZnO cycles followed by 1 AlO_x cycle. Under these deposition cycle conditions, the doping concentration of Al was controlled to be 2.2 at. %. Diethyl zinc ($(C_2H_5)_2Zn$, DEZ) and de-ionized water (H_2O) were used as the precursor reactants for ZnO, while tri-methyl aluminum ($Al(CH_3)_3$, TMA) and H_2O were used for AlO_x. High purity nitrogen (99.999% N_2) gas was used as the purge gas. The pulse times for each DEZ, TMA, and H_2O cycle were 0.1, 0.05, and 0.1 s, respectively, and the N_2 purge time was 8 s. The AZO film thickness target was around 200 nm and the maximum deposition temperature was limited to 260 °C based on the ALD process window. The growth rates per cycle (GPC) of ZnO and AlO_x were calculated from the prepared film thicknesses to be 1.70 and 1.1 Å/cycle at a deposition temperature of 200 °C and 1.66 and 1.09 Å/cycle at 250 °C, respectively.

In order to make use of the TCO as an anode for OLED devices, the prepared AZO films were cleaned using acetone, methanol, H_2O, and isopropyl alcohol in an ultrasonic bath. Then, AZO anodes were patterned by conventional photolithography and were etched over the 2×2 mm^2 emitting area by a wet process using a mixed etchant solution of MA-SO_2 (HCl:HNO_3 based acid solution, Dongwoo Fine-Chem. Cop.):$H_2O = 1{:}10$ for 20 s. OLED devices with a structure of N1, N1′-(biphenyl-4,4′-diyl)bis(N1-phenyl-N4, N4-dimtolyl-benzene-1,4-diamine) [DNTPD, 50 nm]/1,1-bis[(di-4-tolylamino) phenyl] cyclohexane [TAPC, 30 nm]/bis(10-hydroxybenzo [h]quinolinato) beryllium [$Bebq_2$, 30 nm]:10% doped RP-411/4,7-diphenyl-1,10-phenanthroline [Bphen, 50 nm]/LiF [1 nm]/Al [120 nm] were fabricated onto the AZO anode formed by ALD. All organic and cathode materials were deposited by thermal evaporation under a pressure of 5×10^{-6} Torr. DNTPD was used as a hole injection layer (HIL) and effectively reduced the lowest unoccupied molecular orbital energy barrier between the anode and the TAPC hole transport layer. TAPC acted as a hole transport into the emission layer as well as an electron blocking layer with an energy gap 1.0 eV higher than the highest occupied molecular orbital. The electron emission layer (EML) was composed of $Bebq_2$ as a host and RP-411 as a red phosphorescent dopant. Bphen was used as an electron transport layer and hole blocking layer, while LiF/Al was used as the electron injection layer and cathode.

The crystal structure properties of AZO films were analyzed by x-ray diffractometry [(XRD), D/MAX-2000, Rigaku] with Cu $K\alpha_1$ radiation and field emission scanning electron microscopy [(FE-SEM), S-4800, Hitachi]. The optical properties, including the transmittance and UV absorption of the AZO films, were inspected using a UV–visible–near-infrared spectrometer (V-570, Jasco). The electrical properties consisting of the sheet resistance and resistivity of the AZO films were measured using a four-point probe system (Keithley 240) and a Hall effect measurement system (HMS-3000, Ecopia) under 10 mA and a 0.55 T electromagnetic field. The current density, luminance, current efficiency characteristics, and emission spectra of the OLED devices fabricated onto four different TCO anodes were investigated using an I-L-V measurement system (M6100, McScience) in a dark room.

III. RESULTS AND DISCUSSION

Figure 1 shows the x-ray diffraction spectra of the AZO films deposited onto glass substrates at various deposition temperatures ranging from 200 to 260 °C. The main x-ray diffraction spectrum of the ZnO film deposited at 200 °C was observed to have 100, 002, and 110 peaks at 2θ angles of 31.28°, 33.86°, and 56.11°, respectively, with a hexagonal structure.[6,8] The AZO films also showed identical diffraction peaks as the ZnO film. However, upon increasing the deposition temperature from 200 to 260 °C, the AZO films showed a preferred *c*-axis growth orientation, i.e., an increase in the intensity of the 002 diffraction peak, whereas the intensities of the 100 and 110 diffraction peaks gradually decreased and finally vanished at a deposition temperature of 260 °C. This change in growth orientation was suggested to be due to the much smaller ionic radius of Al^{3+} (0.53 Å) than Zn^{2+} (0.74 Å),[15] and therefore this substitutional effect of Al^{3+} ions occupying Zn^{2+} sites can lead to shrinkage of the ZnO lattice. The 002 diffraction peak of AZO deposited at 200 °C moved to a higher diffraction angle than ZnO. The *c*-axis lattice parameters of AZO films fabricated at deposition temperatures of 200, 230, and 260 °C were calculated to be 5.276, 5.258, and 5.252 Å, respectively, which are smaller than the lattice parameter of ZnO (5.290 Å), and which lead us to surmise that higher deposition temperatures enhance the occupation probability of Al^{3+} ions into ZnO. However, the *a*-axis lattice parameters calculated from the 001 diffraction peak of the ZnO film and AZO films deposited at 200 and 230 °C were found to be 3.299, 3.296, and 3.293 Å, respectively, demonstrating a much smaller decrease than the *c*-axis parameter. This enhanced shrinkage along the *c* axis induces a preferred growth orientation along the *c* axis.

The crystallinity of the AZO film also changed with increasing deposition temperature. The *c*-axis grain size of the AZO films increased with increasing deposition temperature compared with the 15.4 nm grain size of the ZnO films deposited at 200 °C. The *c*-axis grain sizes of the AZO films

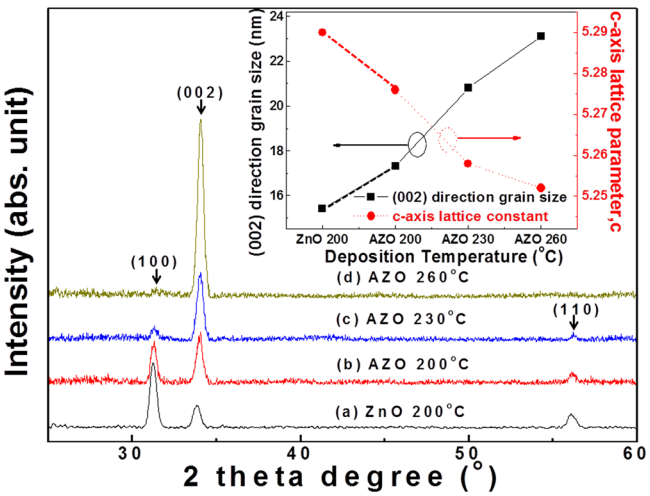

FIG. 1. (Color online) XRD diffraction patterns of the (a) ZnO film deposited at 200 °C and AZO films deposited at (b) 200 °C, (c) 230 °C, and (d) 260 °C. The grain size and *c*-axis lattice constants calculated using the 002 diffraction peak are shown in the inset.

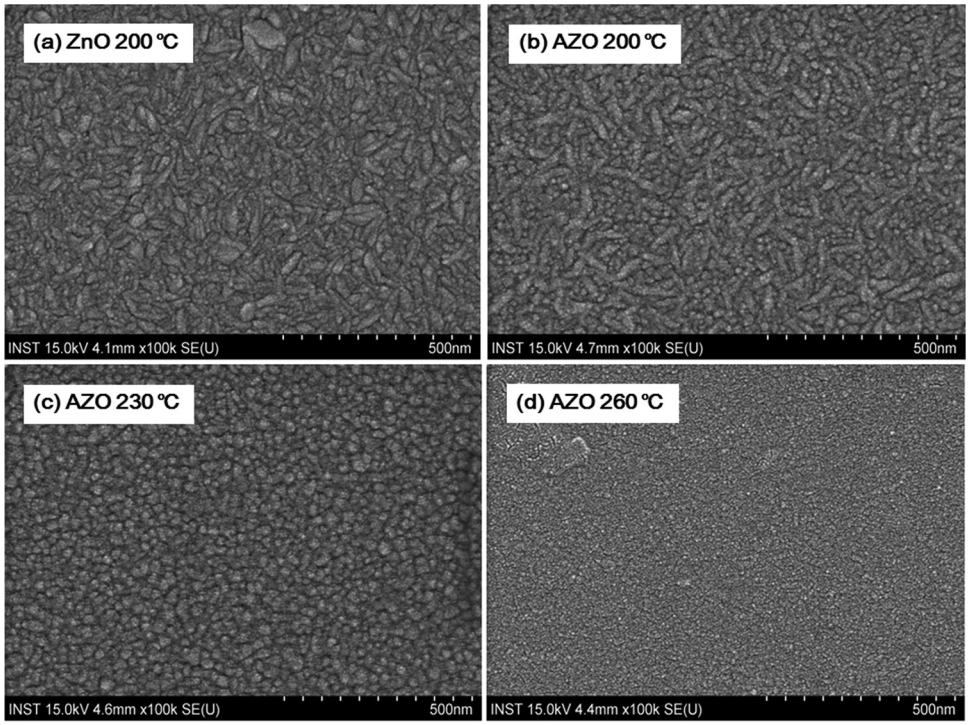

FIG. 2. FE-SEM surface images of the (a) ZnO film deposited at 200 °C and AZO films deposited at (b) 200 °C, (c) 230 °C, and (d) 260 °C.

deposited at temperatures of 200, 230, and 260 °C were calculated using Scherrer's formula to be 17.3, 20.8, and 23.1 nm, respectively.[11] The lattice parameter, c, and grain size of the AZO films deposited at various temperatures are shown in the inset in Fig. 1.

Figure 2 shows the surface morphologies of the ZnO film and AZO films fabricated at deposition temperatures of 200, 230, and 260 °C, as visualized by FE-SEM. The ZnO film deposited at 200 °C had a cylindrical morphology, but the AZO film deposited at 200 °C had a less sharp cylinder particle shape due to the change in the preferred growth orientation along the c axis. The particle shape in the AZO film deposited at 230 °C became almost spherical and the AZO film deposited at 260 °C had a flat and uniform surface morphology with a highly crystalline state, as shown in the XRD pattern in Fig. 1.

Figure 3 shows the electrical properties including the carrier concentration, mobility, and resistivity of the AZO films fabricated at the various deposition temperatures ranging from 200 to 260 °C. All of the prepared AZO films showed n-type semiconductor properties, and the carrier concentration of ZnO deposited by ALD at 200 °C was measured to be $8.44 \times 10^{19}\,\mathrm{cm}^{-3}$, whereas the carrier concentrations of the AZO films increased up to $5.18 \times 10^{20}\,\mathrm{cm}^{-3}$ with increasing deposition temperature. This increasing carrier concentration behavior with increasing deposition temperature agrees well

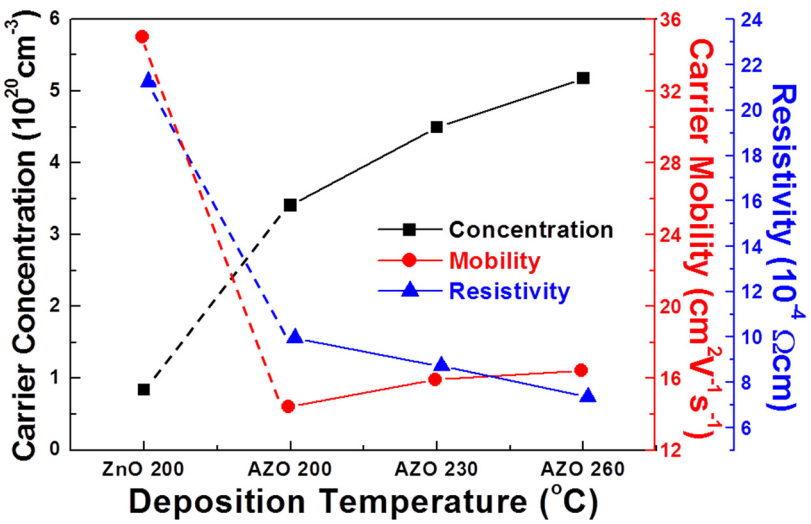

FIG. 3. (Color online) Electrical properties of the ZnO film deposited at 200 °C and AZO films deposited at 200, 230, and 260 °C.

with the decreasing behavior of the *c*-axis parameter, as shown in the XRD spectra in Fig. 1. Otherwise, the carrier mobility of the AZO films decreased compared to ZnO, which appears to be due to the enhanced carrier scattering probability from the substitutional Al^{3+} ions.[16] However, the carrier mobility in the AZO films increased slightly with increasing deposition temperature due to the enhanced crystallinity,[6,14] as shown in Fig. 1. Therefore, the resistivity of the AZO films decreased from 9.94 to 7.34×10^{-4} Ω cm (corresponding average sheet resistances of 93 and 52 Ω/sq) with increasing deposition temperature from 200 to 260 °C.

Figure 4(a) shows the optical transmittance and absorption spectra (inset) in the visible region from 350 to 800 nm and Fig. 4(b) shows plots of the optical bandgap (E_g) vs $(\alpha h\nu)^2$ of the ZnO and AZO films. The average transmittance of the ZnO and AZO films was in the range of 80%–90%. The optical absorption edge for the ZnO and AZO films was determined by extrapolation of the plot of $(\alpha h\nu)^2$ vs E_g, as shown in Fig. 4(b). The optical absorption edge of the AZO films was blueshifted compared to that of the ZnO film, which increased with increasing deposition temperature. Specifically, the E_g value was 3.22 eV for the pure ZnO film and it increased to 3.27, 3.37, and 3.43 eV for the AZO films deposited at 200, 230, and 260 °C, respectively. That is, the Fermi level can be raised with increasing carrier concentration and can be moved into the conduction band. Therefore, the E_g of the AZO film increased with increasing carrier concentration, as observed in Fig. 3. This E_g widening of AZO

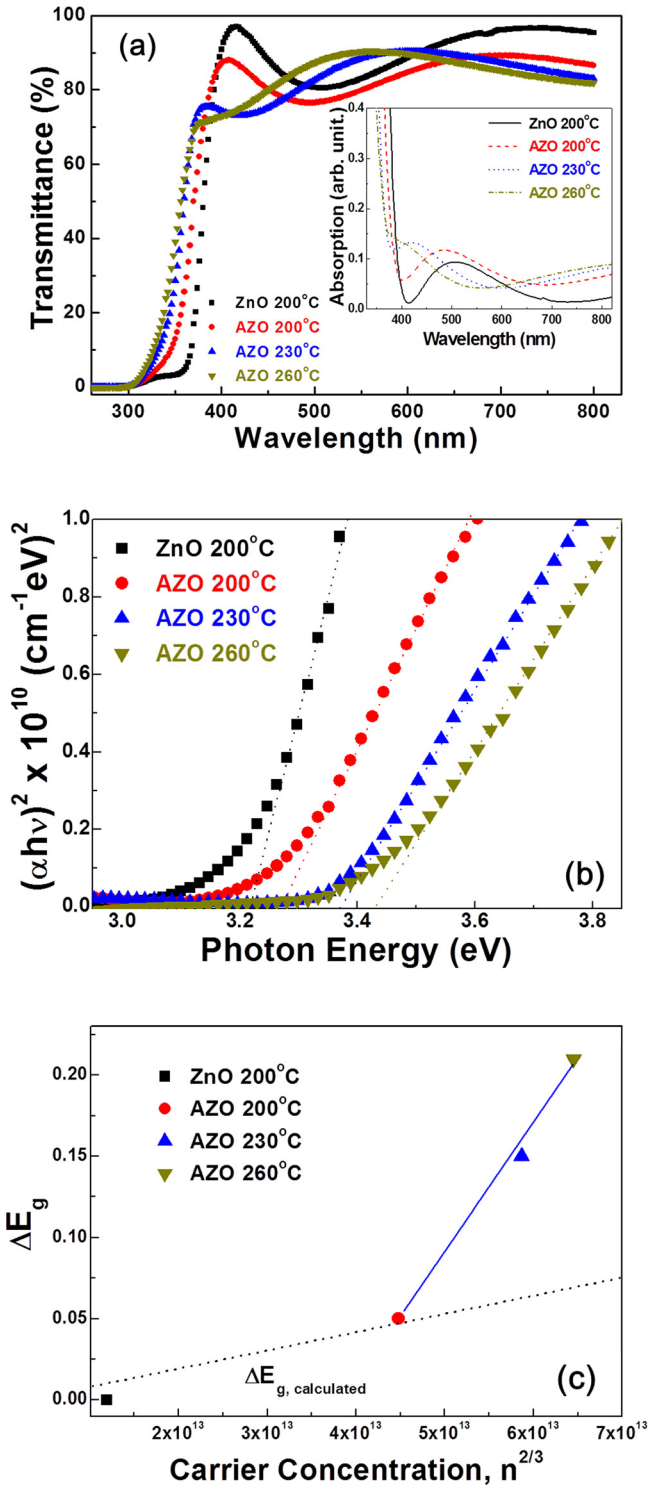

FIG. 4. (Color online) (a) Optical transmittance spectra in the visible range (inset corresponds to absorption behavior), (b) plots of the optical bandgap (E_g) vs $(\alpha h\nu)$,[2] and (c) plots of E_g vs $n^{2/3}$ for the ZnO film deposited at 200 °C and AZO films deposited at 200, 230, and 260 °C.

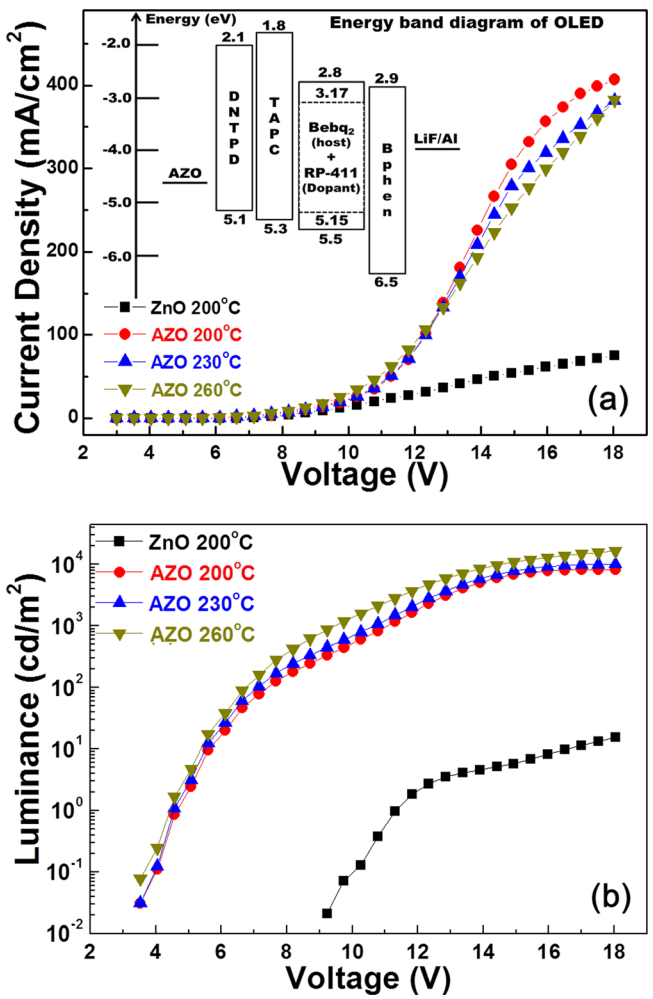

FIG. 5. (Color online) (a) Current density vs voltage (*J*–*V*) characteristics (the inset shows the energy band diagram of the OLED devices) and (b) luminance vs voltage (*L*–*V*) characteristics of the OLED devices with ZnO deposited at 200 °C and AZO deposited at 200, 230, and 260 °C.

TABLE I. Summarized carrier mobility and concentration, resistivity, sheet resistance, transmittance, and figure of merit of pure ZnO film deposited at 200 °C and AZO film deposited at 200, 230, and 260 °C.

Condition	Carrier mobility ($cm^2\ V^{-1}\ s^{-1}$)	Carrier concentration ($\times 10\ cm^{20}$)	Resistivity ($\times 10^{-4}\ \Omega$ cm)	Sheet resistance (Ω/sq)	Transmittance (% at 550 nm)	Figure of merit (in $10^{-3}\ \Omega^{-1}$)
ZnO 200 °C	34.9	0.84	21.25	257	83	0.60
AZO 200 °C	14.4	3.41	9.94	93	80	1.15
AZO 230 °C	15.9	4.49	8.72	79	88	3.53
AZO 260 °C	16.4	5.18	7.34	52	90	6.71

film can be explained by the Burstein–Moss effect,[5,7,8,11–13] as shown as follows:

$$\Delta E_g = \left(\frac{h^2}{2m_{vc}^*}e\right)(3\pi^2)^{2/3}(n)^{2/3}(\text{eV}). \quad (1)$$

In Eq. (1), ΔE_g is the widened optical band edge of the semiconductor with increased carrier concentration, $n^{2/3}$, h is Plank's constant, and m_{vc}^* is the reduced effective mass ($1/m_{vc}^* = 1/m_c^* + 1/m_v^*$). The relationship between ΔE_g and $n^{2/3}$ is shown in Fig. 4(c), where the dashed line corresponds to the calculated Burstein–Moss shift values where $m_c^* = 0.38\,m_o$ and $m_v^* = 1.8\,m_o$. The E_g values of pure ZnO and AZO deposited at 200 °C are in accord with the calculated ΔE_g values. On the other hand, the E_g values of the AZO films deposited at 230 and 260 °C were inconsistent with the $E_g \propto n^{2/3}$ relationship in the Burstein–Moss model. The $n^{2/3}$ value linearly increased with increasing deposition temperature, which can provoke more Al^{3+} ions to diffuse and substitute at Zn^{2+} sites at higher deposition temperatures. As a result, this may influence the crystallinity, surface morphology, and optical properties of the AZO films.

In order to determine the performance of our AZO films as a TCO anode for OLED devices, a figure of merit ($\Phi = T^{10}/R_S$) value was calculated, where T is the optical transmittance at 550 nm and R_S is the sheet resistance, which is a common rating method for TCO films to determine their possible use in optoelectronic applications.[21] The figure of merit values of the AZO films, representing both their electrical and optical properties, are summarized in Table I. The highest figure of merit of the AZO films was $6.71 \times 10^{-3}\ \Omega^{-1}$ for the film deposited at 260 °C, which had the lowest sheet resistance and highest optical transmittance.

Figure 5(a) shows the current density versus voltage (J–V) and Fig. 5(b) shows the luminance versus voltage (L–V) characteristics of the OLED devices with ZnO and AZO anodes. The schematic energy band of the OLED devices with the AZO/DNTPD/TAPC/Bebq$_2$:10% doped RP-411/Bphen/LiF/Al structure is presented in the inset in Fig. 5(a). The OLED device with the ZnO anode showed lower current density and luminance characteristics, while the maximum luminance value was found to be 15 cd/m^2 at 18 V. The maximum current density value for the OLED test device with ZnO was 72 mA/cm^2, whereas the OLEDs with AZO anodes all had similar maximum current densities of approximately 400 mA/cm^2. The maximum luminance values of the OLED devices with AZO anodes deposited at 200, 230, and 260 °C increased to 8296, 11 210, and 16 680 cd/m^2 (at 18 V), respectively. On the other hand, the turn-on voltage (at 10 cd/m^2) of the OLED devices decreased to 5.7, 5.4, and 5.3 V with increasing deposition temperature. From the luminance and current density results, the current efficiency was calculated, and the current efficiency versus current density (η_c–J) characteristics of the OLED devices with ZnO and AZO anodes are shown in Fig. 6. The current efficiency of the device with the ZnO anode was nearly zero. The maximum current efficiencies in the turn-on voltage region of the OLED devices with AZO anodes grown at deposition temperatures of 200, 230, and 260 °C were 2.3, 2.9, and 4.4 cd/A, respectively. The lowest turn-on voltage and the highest luminance and current efficiency values were obtained for the device with the AZO anode deposited at 260 °C, corresponding to the AZO film with the lowest sheet resistance and highest optical transmittance. These results can be correlated with the figure of merit values of the AZO films. With decreasing figure of merit values of the AZO TCOs, the luminance and current efficiency values of the OLED device increased, as shown in Table I. Another factor to consider is the work function of the anode, which is one of the key issues for improving the electrical and optical characteristics of OLED devices, since a lower energy barrier between the anode and HIL layer can allow the carrier transmission to occur more easily and effectively. The work function of the ZnO film is 3.74 eV.[20] Jiang *et al.* reported a

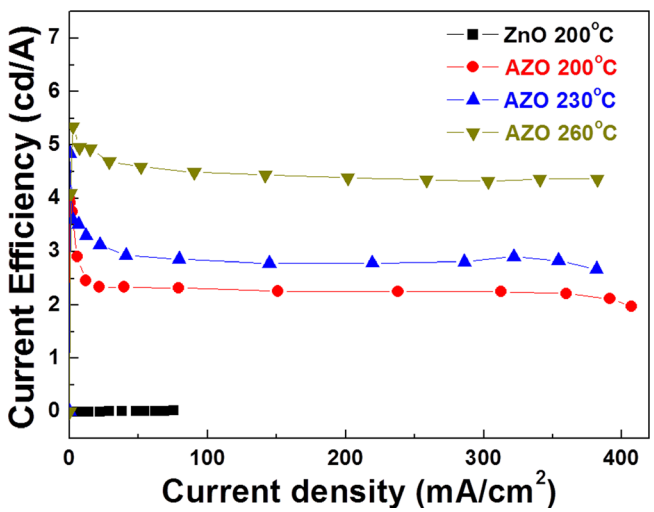

FIG. 6. (Color online) Current efficiency vs current density (η_c–J) characteristics of the OLED devices containing ZnO deposited at 200 °C and AZO deposited at 200, 230, and 260 °C.

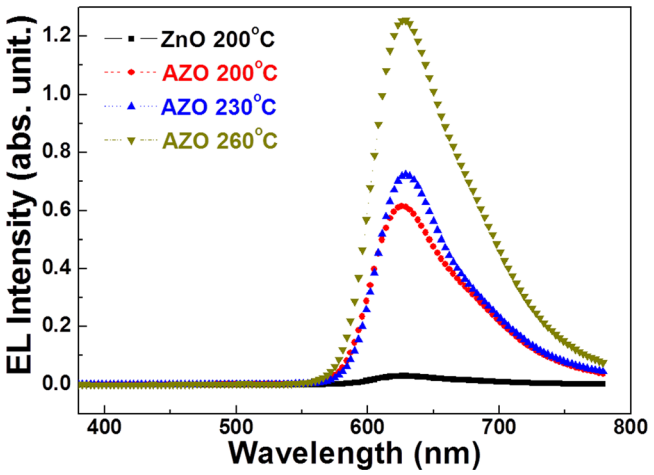

FIG. 7. (Color online) EL efficiency of the OLED devices containing ZnO deposited at 200 °C and AZO deposited at 200, 230, and 260 °C.

work function of 4.4 eV of AZO films doped with 2.1 at. % Al by a sputtering method,[9] and Meyer *et al.* reported the work function of AZO films deposited by the ALD method to be 4.2 eV.[18] Therefore, the hole injection barrier between the AZO anode and DNTPD is lower than that of a ZnO anode. Accordingly, in the case of OLED devices with AZO anodes, the hole injection into the DNTPD was greater than in the case of OLEDs with a pure ZnO anode because a large amount of hole–electron (exciton) recombination was generated within the $Bebq_2$:RP-411 EML. Therefore, the OLED devices with AZO anodes show a higher luminance and current efficiency than those with a ZnO anode due to their reduced sheet resistance and hole injection barrier.

Figure 7 shows the electroluminescence (EL) characteristics of OLED devices with ZnO and AZO anodes at maximum luminance. All prepared OLED devices showed good red emission and their EL intensity was consistent with their luminance. The main peaks of the EL spectra of the OLED devices with AZO anodes deposited at temperatures ranging from 200 to 260 °C were slightly shifted from 623 to 628 nm, which also agrees well with the absorption behavior shown in the inset in Fig. 4(a).

IV. CONCLUSION

In this work, AZO films deposited at various temperatures by the ALD method were studied for use as TCO anodes in OLED devices. The AZO films showed enhanced electrical conduction with increasing deposition temperature because the electron carrier concentration increased due to successful substitution of Zn^{2+} with Al^{3+}. The best transmittance and resistivity results were 90% and 7.34×10^{-4} Ω cm, respectively, found in the AZO film deposited at 260 °C, corresponding to the best figure of merit. Consequently, the best performance of the OLED devices was achieved with this AZO anode material where the maximum luminance and current efficiency values were 16 680 cd/m^2 and 4.4 cd/A, respectively. From these results, it can be concluded that AZO films deposited by ALD at a controlled deposition temperature are a promising electrode material for low-temperature-deposition OLED devices.

ACKNOWLEDGMENTS

This work was supported by the Industrial Strategic Technology Development Program (Grant No. 10041926) funded by the Ministry of Knowledge Economy (MKE, Korea). S.C.G. is very grateful to the Brain Korea office for financial support provided through a post-doctorate fellowship.

[1]D. Xu, Z. Deng, Y. Xu, J. Xiao, C. Liang, Z. Pei, and C. Sun, Phys. Lett. A **346**, 148 (2005).
[2]L. Gong, Z. Ye, J. Lu, L. Zhu, J. Huang, X. Gu, and B. Zhao, Vacuum **84**, 947 (2010).
[3]C. E. Kim, P. Moon, I. Yun, S. Kim, J.-M. Myoung, H. W. Jang, and J. Bang, Expert Sys. Applic. **38**, 2823 (2011).
[4]Y. R. Park, E. Nam, J.-H. Boo, D. Jung, S. J. Suh, and Y. S. Kim, Bull. Korean Chem. Soc. **28**, 2396 (2007).
[5]A. Di Trolio, E. M. Bauer, G. Scavia, and C. Veroli, J. Appl. Phys. **105**, 113109 (2009).
[6]H. Tanaka, K. Ihara, T. Miyata, H. Sato, and T. Minami, J. Vac. Sci. Technol. A **22**, 1757 (2004).
[7]S.-M. Park, T. Ikegami, K. Ebihara, and P.-K. Shin, Appl. Surf. Sci. **253**, 1522 (2006).
[8]J. H. Park, J. M. Shin, S.-Y. Cha, J. W. Park, S.-Y. Jeong, H. K. Pak, and C.-R. Cho, J. Korean Phys. Soc. **49**, S584 (2006).
[9]X. Jiang, F. L. Wong, M. K. Fung, and S. T. Lee, Appl. Phys. Lett. **83**, 1875 (2003).
[10]D.-J. Yun and S.-W. Rhee, Thin Solid Films **517**, 4644 (2009).
[11]S. Mridha and D. Basak, J. Phys. D: Appl. Phys. **40**, 6902 (2007).
[12]T. Dhakal, D. Vanhart, R. Christian, A. Nandur, A. Sharma, and C. R. Westgate, J. Vac. Sci. Technol. A **30**, 021202 (2012).
[13]P. Banerjee, W.-J. Lee, K.-R. Bae, S. B. Lee, and G. W. Rubloff, J. Appl. Phys. **108**, 043504 (2010).
[14]W. J. Maeng, J.-W. Lee, J. H. Lee, K.-B. Chung, and J.-S. Park, J. Phys. D: Appl. Phys. **44**, 445305 (2011).
[15]N. P. Dasgupta, S. Neubert, W. Lee, O. Trejo, J.-R. Lee, and F. B. Prinz, Chem. Mater. **22**, 4769 (2010).
[16]S. J. Lim, S. K. Lee, M. Jo, C.-S. Lee, S. Kwon, and H. Kim, J. Korean Phys. Soc. **53**, 253 (2008).
[17]H. Saarenpää, T. Niemi, A. Tukiainen, H. Lemmetyinen, and N. Tkachenko, Sol. Energy Mater. Sol. Cells **94**, 1379 (2010).
[18]J. Meyer, P. Görrn, S. Hamwi, H.-H. Johannes, T. Riedl, and W. Kowalsky, Appl. Phys. Lett. **93**, 073308 (2008).
[19]S.-H. K. Park, C.-S. Hwang, H. Y. Jeong, H. Y. Chu, and K. I. Cho, Electrochem. Solid State Lett. **11**, H10 (2008).
[20]S. M. George, Chem. Rev. **110**, 111 (2010).
[21]G. Haacke, J. Appl. Phys. **47**, 4086 (1976).